SUPPORTING INFORMATION

Sustainably closed loop recycling of hierarchically porous polymer microbeads for efficient removal of cationic dyes

Jikang Li[a#], Qin Yang[a#], Sheng Chen[a], Kerry McPhedran[b,c], Yingchun Gu[a], Rongfu Huang[d*], Bin Yan[a*]

[a] National Engineering Laboratory for Clean Technology of Leather Manufacture, College of Biomass Science and Engineering, Sichuan University, Chengdu, 610065, China

[b] Department of Civil, Geological & Environmental Engineering, College of Engineering, University of Saskatchewan, Saskatoon, SK, Canada

[c] Global Institute for Water Security, University of Saskatchewan, Saskatoon, SK, Canada

[d] MOE Key Laboratory of Deep Earth Science and Engineering, College of Architecture and Environment, Sichuan University, Chengdu, Sichuan 610065, China

Section S.1 Standard curves of three cationic dyes

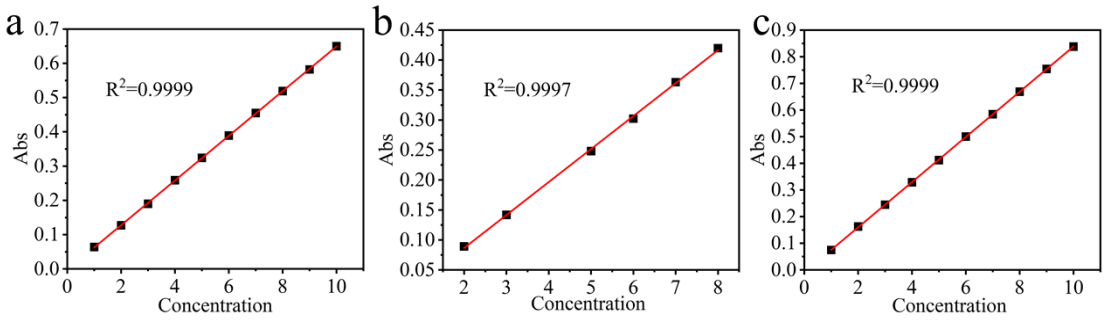

Fig. S1 Standard curve of cationic dyes: (a) Methylene blue; (b) Malachite green; (c) Methyl violet 2B.

The equation obtained by curve fitting.

Methylene blue: A=0.0652c-0.0027 (1)

Malachite green: A=0.055c-0.0234 (2)

Methyl vioiet 2B: A=0.0848c-0.0094 (3)

A is the absorbance of the solution, and C(mg/L) is the concentration of the solution.

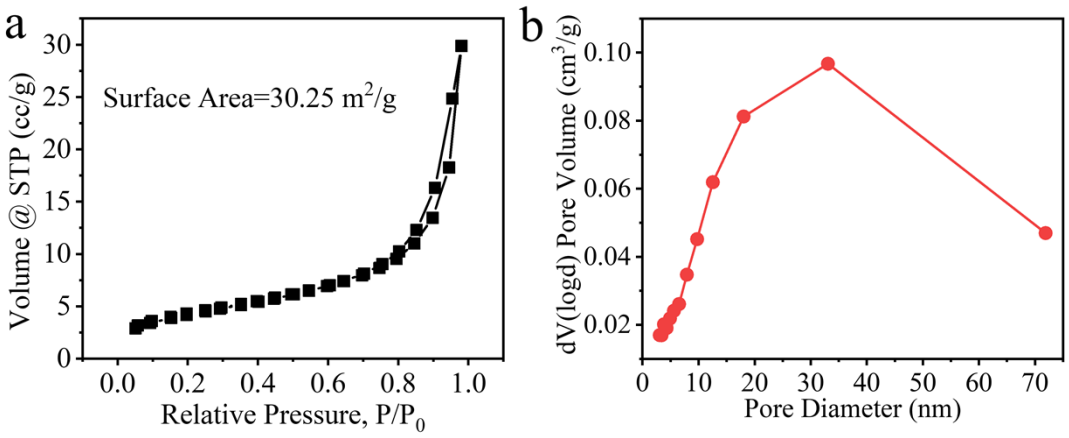

Fig. S2. (a) Nitrogen adsorption–desorption isotherm obtained for PCP-IDA adsorbents; (b) Pore size Distribution of PCP-IDA.

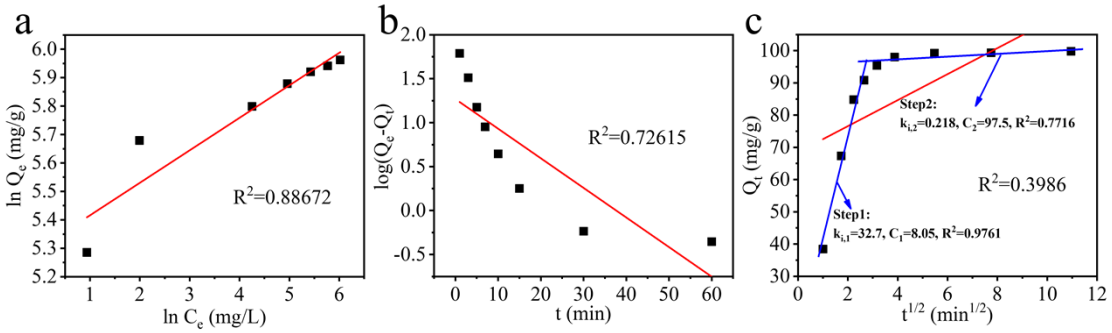

Fig. S3. (a) Freundlich fitting curve in isothermal adsorption model. (b)The fitting result of the pseudo-first-order model; (c) The fitting result of the intra-particle diffusion kinetic model.

Table S1. Estimated values of parameters for different kinetic models.

Kinetic model	Parameters		
Pseudo-first-order	Q_e(mg·g^{-1})	k_1(mg·g^{-1})	R^2
	99.8	0.776	0.72615
Pseudo-second-order	Q_e(mg·g^{-1})	k_2(g·mg^{-1}·min^{-1})	R^2
	101.01	0.1077	0.99988
Intra-particle diffusion	C(mg·g^{-1})	k_i(mg·g^{-1}·min$^{-1/2}$)	R^2
	68.514	4.0339	0.39864

Table S2. Isothermal adsorption fitting curve data.

Langmuir			Freundlich		
Q_m(mg/g)	K_L(L/mg)	R^2	n	K_F(L/mg)	R^2
384.62	0.1354	0.99897	8.7489	200.68	0.88672

182

183 **Table S3**. The comparison of the adsorption capacity of PCP-IDA adsorbent with other reported

184 adsorbents with similar structure or size.

Adsorbent/mass	MB concentration/ volume	pH	Temperature	Adsorption capacity (mg/g)	Kinetic (min)	References
Nanocomposites poly(GDMA)/MCM-41/20 mg	40 mg/L 40 mL	6	Room temperature	MB: 111.11	20	[1]
MAA/GMA-g-PET fibers/100 mg	40 mg/L 25mL	10	298K	MB: 52.1	60	[2]
Cell-g-AASO3H-co-GMA/50 mg	20 mg/L 50 mL	7	298K	MG: 46.23 MV: 53.53	120	[3]
Poly GMA/DVB/200 mg	5 mg/L 25 mL	7	Room temperature	MG: 13.6	50	[4]
MCTSms-PMAA/4.5 mg	200 mg/L 40 mL	12	Room temperature	MB: 211.11	100	[5]
ATP@CCS/7.5 mg	200 mg/L 20 mL	10	298.15K	MB: 215.73	120	[6]
PES/GO porous particles/5 mg	150 μmol/L 20mL	7	303K	MB: 62.5	3600	[7]
UiO-66/MIL-101(Fe)/10 mg	50 mg/L 20mL	9	298K	MB: 448.71	30	[8]
A/γ-Fe_2O_3/f-CNT composite beads/50 mg	230 mg/L 50 mL	5.2	298K	MB: 396.7	2880	[9]
MPGB biosorbent/50 mg	50 mg/L 100mL	7	293K	MB: 231.5	60	[10]
P(G-E)@IDA/10 mg	100 mg/L 10 mL	7	298K	MB: 384.62 MG: 333.33 MV: 322.58	15	In this work

185

186

187

188

189

190

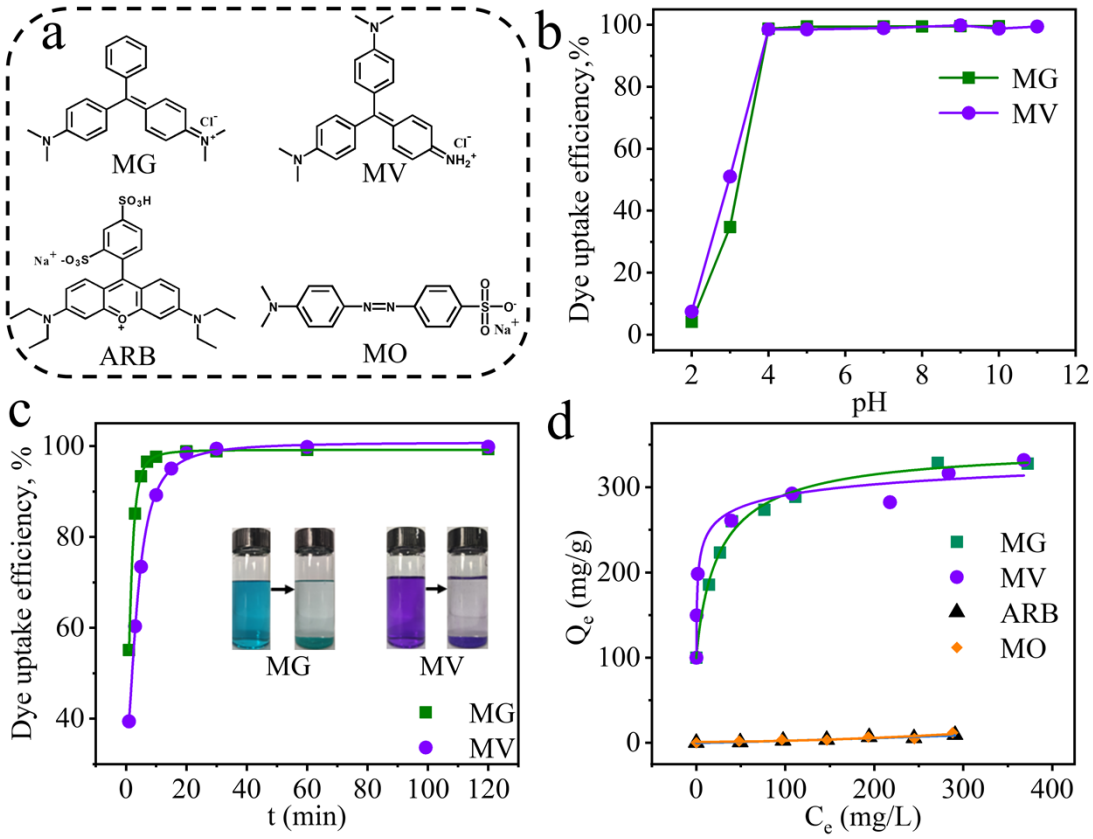

Fig. S4. (a) The chemical structure of MG, MV, ARB and MO dyes; (b) Effect of initial PH of dye solution on adsorption; (c) Rapid adsorption of MG and MV dyes; (d) The equilibrium adsorption capacity of four dyes by PCP-IDA adsorbent.

Section S.2 The related models and parameters of PCP-IDA adsorbent for MG and MV dye adsorption were fitted.

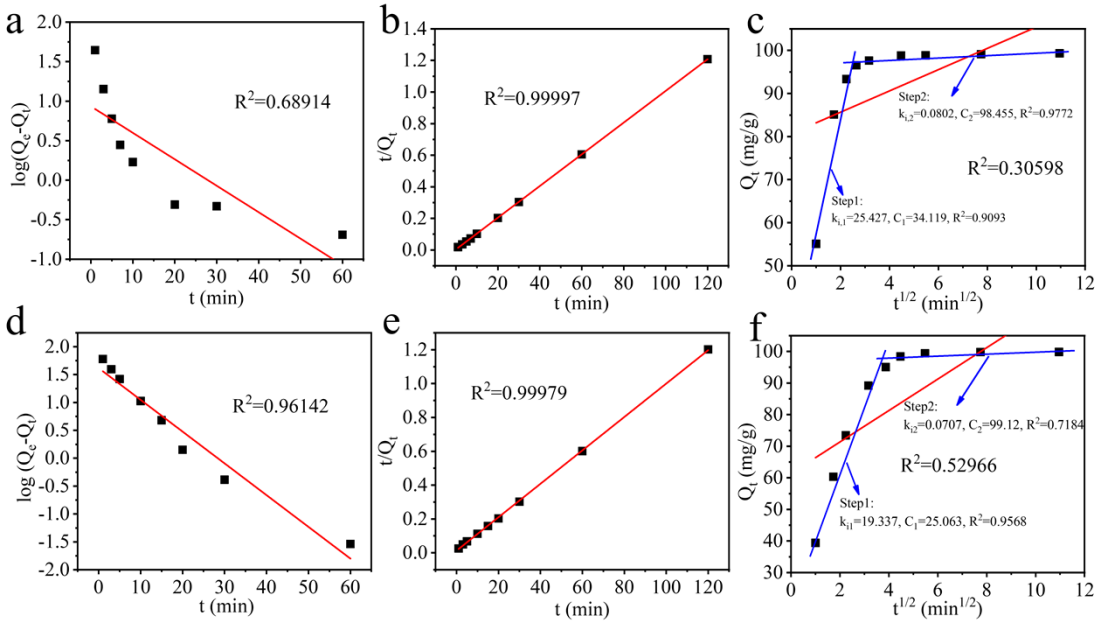

Fig. S5. (a) Pseudo-first-order model of MG; (b) Pseudo-second-order model of MG; (c) Intra-particle diffusion model of MG; (d) Pseudo-first-order model of MV; (e) Pseudo-second-order model of MV; (f) Intra-particle diffusion model of MV.

Table S4. Estimated values of parameters for different kinetic models.

Dye	Kinetic model	Parameters		
MG	Pseudo-first-order	Q_e(mg·g^{-1})	k_1(mg·g^{-1})	R^2
		99.32	0.0772	0.68914
	Pseudo-second-order	Q_e(mg·g^{-1})	k_2(g·mg^{-1}·min^{-1})	R^2
		100	0.025	0.99997
	Intra-particle diffusion	C(mg·g^{-1})	k_i(mg·g^{-1}·min$^{-1/2}$)	R^2
		78.891	2.6216	0.30598
MV 2B	Pseudo-first-order	Q_e(mg·g^{-1})	k_1(mg·g^{-1})	R^2
		99.8361	0.1313	0.96142
	Pseudo-second-order	Q_e(mg·g^{-1})	k_2(g·mg^{-1}·min^{-1})	R^2
		101.01	0.0076	0.99979
	Intra-particle diffusion	C(mg·g^{-1})	k_i(mg·g^{-1}·min$^{-1/2}$)	R^2
		61.408	4.7948	0.52966

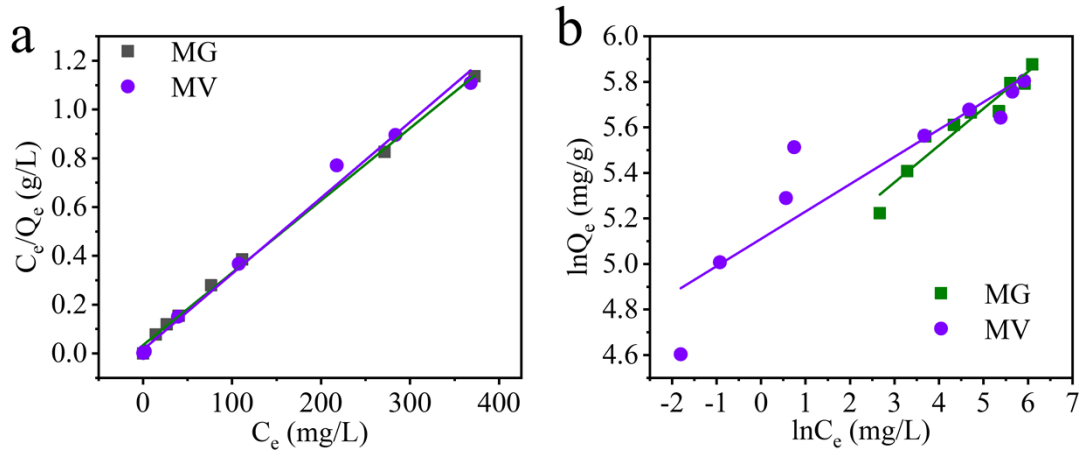

Fig. S6. The fitting model of isothermal adsorption of MG and MV dyes: (a) Langmuir model; (b) Freundlich models.

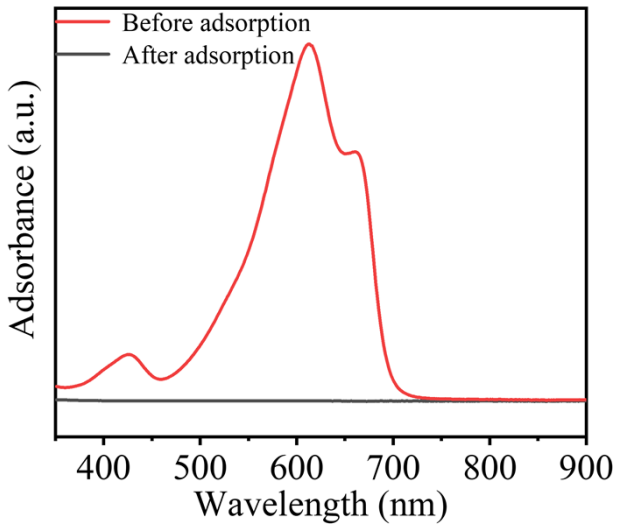

Fig. S7. Adsorption of mixed dye solution of MB, MG and MV.

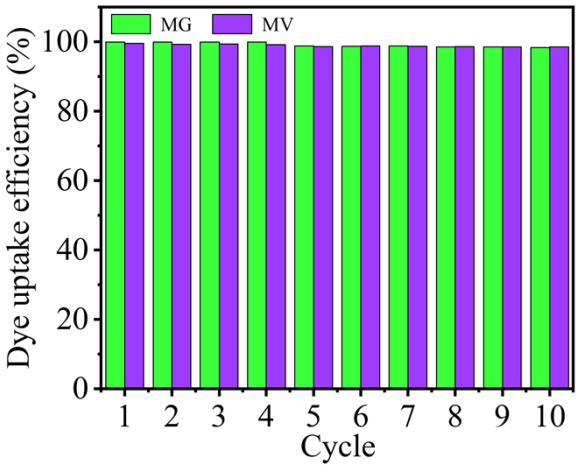

Fig. S8. The cyclic adsorption performance of PCP-IDA adsorbent for MG and MV dyes.

Reference

1. Z. Cherifi, B. Boukoussa, A. Mokhtar, M. Hachemaoui, F. Z. Zeggai, A. Zaoui, K. Bachari and R. Meghabar, Preparation of new nanocomposite poly(GDMA)/mesoporous silica and its adsorption behavior towards cationic dye, *React. Funct. Polym.*, 2020, **153**, 104611.
2. M. Arslan, Preparation and Application of Glycidyl Methacrylate and Methacrylic Acid Monomer Mixture-Grafted Poly(ethylene terephthalate) Fibers for Removal of Methylene Blue from Aqueous Solution, *J. Appl. Polym. Sci.*, 2011, **119**, 3034-3042.
3. R. K. Sharma and R. Kumar, Functionalized cellulose with hydroxyethyl methacrylate and glycidyl methacrylate for metal ions and dye adsorption applications, *Int. J. Biol. Macromol.*, 2019, **134**, 704-721.
4. D. Husaain, M. Najam-ul-Haq, A. Saeed, F. Jabeen, M. Athar and M. N. Ashiq, Synthesis of poly GMA/DVB and its application for the removal of Malachite Green from aqueous medium by adsorption process, *Desalin. Water Treat.*, 2015, **53**, 2518-2528.
5. S. Y. Yu, J. L. Cui, H. Jiang, C. S. Zhong and J. Meng, Facile fabrication of functional chitosan microspheres and study on their effective cationic/anionic dyes removal from aqueous solution, *Int. J. Biol. Macromol.*, 2019, **134**, 830-837.
6. Q. Zhou, Q. Gao, W. J. Luo, C. J. Yan, Z. N. Ji and P. Duan, One-step synthesis of amino-functionalized attapulgite clay nanoparticles adsorbent by hydrothermal carbonization of chitosan for removal of methylene blue from wastewater, *Colloid Surf. A*, 2015, **470**, 248-257.
7. X. Zhang, C. Cheng, J. Zhao, L. Ma, S. D. Sun and C. S. Zhao, Polyethersulfone enwrapped graphene oxide porous particles for water treatment, *Chem. Eng. J.*, 2013, **215**, 72-81.
8. A. S. Eltaweil, E. M. Abd El-Monaem, G. M. El-Subruiti, M. M. Abd El-Latif and A. M. Omer, Fabrication of UiO-66/MIL-101(Fe) binary MOF/carboxylated-GO composite for adsorptive removal of methylene blue dye from aqueous solutions, *RSC Adv.*, 2020, **10**, 19008-19019.
9. S. Alvarez-Torrellas, M. Boutahala, N. Boukhalfa and M. Munoz, Effective Adsorption of Methylene Blue dye onto Magnetic Nanocomposites. Modeling and Reuse Studies, *Appl. Sci-Basel.*, 2019, **9**, 4563.
10. C. Li, X. J. Wang, D. Y. Meng and L. Zhou, Facile synthesis of low-cost magnetic biosorbent from peach gum polysaccharide for selective and efficient removal of cationic dyes, *Int. J. Biol. Macromol.*, 2018, **107**, 1871-1878.